A new regime that “FIRE”s fusion plasmas for long sustained and high performance reactor conditions

Yong-Su Na (ysna@snu.ac.kr)
Seoul National University https://orcid.org/0000-0001-7270-3846

Hyunsun Han
Korea Institute of Fusion Energy

Sangjin Park
Seoul National University https://orcid.org/0000-0002-4453-0439

Jisung Kang
Korea Institute of Fusion Energy

Young-Ho Lee
Korea Institute of Fusion Energy

Jinil Jung
Korea Institute of Fusion Energy

Minsoo Cha
Department of Nuclear Engineering, Seoul National University

Gyungjin Choi
Department of Nuclear Engineering, Seoul National University

Minjun Choi
Korea Institute of Fusion Energy

Jinwoo Gwak
Department of Nuclear Engineering, Seoul National University

Taik Soo Hahm
Seoul National University

Sang Hee Hahn
Korea Institute of Fusion Energy https://orcid.org/0000-0001-8115-9248

Juhyeok Jang
Korea Institute of Fusion Energy

Kwan Chul Lee
Korea Institute of Fusion Energy

Boseong Kim
Department of Nuclear Engineering, Seoul National University

Junghee Kim
Korea Institute of Fusion Energy

SangKyeun Kim

Princeton Plasma Physics Laboratory
Woong Chae Kim
Korea Institute of Fusion Energy
Jinseok Ko
Korea Institute of Fusion Energy
Wonha Ko
Korea Institute of Fusion Energy
Chanyoung Lee
Department of Nuclear Engineering, Seoul National University
Jaehyun Lee
Korea Institute of Fusion Energy
Jekil Lee
Korea Institute of Fusion Energy
Jungpyo Lee
Department of Nuclear Engineering, Hanyang University
Kyu-Dong Lee
Korea Institute of Fusion Energy
Jong-Kyu Park
Princeton Plasma Physics Laboratory
Young-Seok Park
Department of Applied Physics and Applied Mathematics, Columbia University
Jaemin Seo
Department of Nuclear Engineering, Seoul National University
Choongki Sung
Department of Nuclear and Quantum Engineering, Korea Advanced Institute of Science and Technology
SeongMoo Yang
Princeton Plasma Physics Laboratory
Siwoo Yoon
Korea Institute of Fusion Energy

Physical Sciences - Article

Keywords: fusion plasma, nuclear fusion, fast ion roled enhancement

Posted Date: October 11th, 2021

DOI: https://doi.org/10.21203/rs.3.rs-935325/v1

Version of Record: A version of this preprint was published at Nature on September 7th, 2022. See the published version at https://doi.org/10.1038/s41586-022-05008-1.

Abstract

We report a discovery of a fusion plasma regime suitable for commercial fusion reactor where the ion temperature was sustained above 100 million degree about 20 s for the first time. Nuclear fusion as a promising technology for replacing carbon-dependent energy sources has currently many issues to be resolved to enable its large-scale use as a sustainable energy source. State-of-the-art fusion reactors cannot yet achieve the high levels of fusion performance, high temperature, and absence of instabilities required for steady-state operation for a long period of time on the order of hundreds of seconds. This is a pressing challenge within the field, as the development of methods that would enable such capabilities is essential for the successful construction of commercial fusion reactor. Here, a new plasma confinement regime called fast ion roled enhancement (FIRE) mode is presented. This mode is realized at Korea Superconducting Tokamak Advanced Research (KSTAR) and subsequently characterized to show that it meets most of the requirements for fusion reactor commercialization. Through a comparison to other well-known plasma confinement regimes, the favourable properties of FIRE mode are further elucidated and concluded that the novelty lies in the high fraction of fast ions, which acts to stabilize turbulence and achieve steady-state operation for up to 20 s by self-organization. We propose this mode as a promising path towards commercial fusion reactors.

Background

With the current focus on achieving carbon neutrality, nuclear fusion has drawn more attention because it does not produce carbon dioxide during power generation and does not generate high-level radioactive waste[1]. To obtain massive electricity from nuclear fusion reactor economically, plasmas with high fusion performance in steady-state conditions for long pulse durations must be maintained. To accomplish this, we should make a plasma in which the fusion reaction occurred frequently from i) high energy and particle confinement for high fusion performance, and ii) a high ion temperature above 100 million Kelvin for the high fusion reaction cross-section. Simultaneously, the plasma should be stable iii) without severe plasma instabilities damaging the device at high plasma pressure, and be sustained as steady-state by iv) a fully noninductive current drive vi) without impurity accumulation[2]. Since 1950s, the tokamak device has been developed and considered as the first option to confine the plasma for nuclear fusion, however, no tokamak plasma operation mode realised thus far satisfies all the above requirements.

In the 1980s, a confinement regime so-called 'H-mode[3]' which relies on confinement improvement at the edge region of the plasma has been developed and becomes mainstream for the tokamak study. In H-mode, the plasma turbulence at the edge region is stabilised, resulting in the formation of edge transport barriers (ETBs). H-mode is considered the reference scenario to produce a fusion power of 500 MW with a fusion gain Q = 10, implying a fusion power ten times higher than the input heating power, in the International Thermonuclear Experimental Reactor (ITER)[4], which is the world's largest tokamak being built in France under a collaboration between China, the EU, India, Japan, the Republic of Korea, Russia, and the U.S.A.[5-7]. Various advanced tokamak operation modes such as hybrid mode[8,9], high poloidal beta

mode[10], and high q_{min} mode[11] are based on this H-mode. H-modes can satisfy the high confinement and avoid impurity accumulation for a long pulse duration[12,13], but their large pressure gradient at the edge due to ETBs triggers a significant edge plasma instability, the so-called edge localised mode (ELM), which can severely damage the inner wall of the device[14,15]. Therefore, vigorous efforts are being made to develop robust methods to control ELM[13,16-22], and plasma control has become more complex. As one of the alternative scenarios for the H-modes, internal transport barrier (ITB) discharges, relying on confinement improvement at the core region, rather than the edge region, resulting from core turbulence suppression[23,24], could satisfy many of the criteria mentioned above. However, these discharges cannot be sustained for a long time due to severe instabilities and impurity accumulation[25-30]. Due to these difficulties, ITER has not been able to offer a robust advanced scenario, beyond the basic mission, to accomplish steady-state operations relevant to a demonstration fusion power plant, DEMO.

Recently, we established a new confinement regime by combining the advantages of scenarios based on the H-mode and ITB to satisfy the requirements described above in Korea Superconducting Tokamak Advanced Research (KSTAR)[31]. We have tried to form ITB in support of fast ions at low density and avoid H-mode transition at the edge region in the diverted plasma configuration as described in Experimental Approach in the Methods. This new plasma regime achieved, for the first time, an ion temperature over 10 keV (~120 million Kelvin) at the centre of the plasma for about 20 s, as shown in Fig. 1a and Extended Data Movie 1.

Fig. 1b-i shows the time evolution of the main physics and engineering parameters for a representative discharge of this regime in KSTAR which demonstrates that this new regime can satisfy most of the requirements of commercial fusion reactors. First, the energy confinement is comparable to that of a conventional H-mode. The energy confinement enhancement factor relative to the ITER89P scaling law[32], H_{89}, is close to or above 2 (Fig. 1c), implying that the energy confinement time is similar with that of H-modes, typically showing H_{89}~2. On the contrary, the particle confinement is not enhanced, resulting in a low plasma density (Fig. 1d). This is a key to prevent the ELM and low impurity accumulation. Second, the plasma temperatures are high, especially the ion temperature, which is important to the high cross-section for fusion reaction, is above 10 keV (Fig. 1e). Third, D_α signal spikes which notify the ELMs are observed, is not observed as shown in Fig. 1f, indicating no considerable particle or heat flux from the plasma to the wall due to ELMs. Consequently, this mode can help improve the lifetime of the plasma-facing component of a fusion reactor by preventing this heat and particle flux-induced damage. Fourth, a close to fully noninductive current drive is obtained. As shown in Fig. 1g, the loop voltage, defined as the voltage created in an external circular loop concentric with the plasma column, is sustained at ~0.1 V. This low voltage means a high probability of operating steady-state conditions since the current sustained by the external current loop is minimised due to its flux reserves. Fifth, this regime was sustained for approximately 20 s by self-organization so that no additional delicate feedback control is needed. Most of the advanced tokamak operation modes requires a sophisticated plasma control schemes, such as pressure- or q-profile control[33], where q is the safety factor. Once the plasma enters this

new regime, however, the plasma is sustained stationary without severe instabilities such as pressure-driven instabilities[34,35] and/or abrupt plasma disruptions[36,37]. Note that abrupt plasma disruption is one of the critical issues in fusion plasmas and the highest priority research topic in ITER[38,39]. The plasma in this regime shows relatively high internal inductance (li) such that it maintains a high plasma pressure (β_N) against plasma instabilities[40], where li is the plasma internal inductance and β_N is the plasma pressure normalised to the magnetic pressure. It is noteworthy that an instability is observed, as indicated by the abrupt decay of the central ion temperature and the corresponding magnetic field fluctuations in the Mirnov coil signal at approximately 6.5 s (Fig. 1h). This instability can also be identified by the outstanding sound transformed from various diagnostic signals in Extended Data Movie 1. However, its impact on the total stored plasma energy, W_{MHD}, is small, as seen in Fig. 1c, because the instability is located in a small volume of the central region of the plasma. Lastly, Fig. 1i shows that the impurity carbon III line stays more or less constant during the whole discharge. Therefore, no notable impurity accumulation is observed and no severe dilution by impurities is foreseen.

We coined this regime to the fast ion roled enhancement (FIRE) mode and now address the reason for the naming by demonstrating the factors for the improvements. We can evaluate the origin of the enhancement of the FIRE mode by comparing it with another confinement mode that shows comparable performance. A 'hybrid mode' is selected for this comparison[8], which can be categorised into H-modes but with higher performance. It is an alternative high-performance scenario for substituting the H-mode in ITER for engineering tests of reactor-relevant components[9] and is considered a candidate operation scenario for DEMO[41,42]. Fig. 2 compares the main parameters between the two confinement modes. As shown in Fig. 2a, they exhibit almost identical operating conditions in terms of the plasma current, magnetic field strength, and heating power, with the only exception being the plasma configuration. The null magnetic vector potential where the magnetic field lines intersect in the plasma configuration is located on the upper region of the plasma, upper single null (USN) in the FIRE mode but on the lower region of the plasma, lower single null (LSN) in the hybrid mode as shown in Fig. 2b. Their performance is very similar in the high heating phase of 5 to 8 s, as represented by $\beta_N < 2.6$ and $H_{89} < 2.3$. Note that conventional H-modes typically exhibit $\beta_N < 2.0$ and $H_{89} \sim 2.0$ in KSTAR[43]. Despite their similar performance, the evolutions of the plasma density are very different. This results from different plasma configurations as described in Experimental Approach in the Methods. The hybrid mode entered the H-mode at approximately 1.8 s, as indicated by the abrupt increases in the performance and density. In contrast, the FIRE mode avoids the H-mode transition over the entire discharge. This is clearly seen in the radial profiles of density and temperature in Fig. 2c. The steep gradients at the edge region, ETB as an indicator of H-modes are seen in all the transport channels of the hybrid mode but not in the FIRE mode. Instead, large gradients exist in the core region of the ion temperature in the FIRE mode. This large gradient region corresponds to ITB. As described in the Methods, this large gradient region exhibits the ITB characteristic, a bifurcation in the energy transport resulting from turbulence stabilisation, which was identified along with inverse ion temperature gradient (ITG) lengths above the critical value of ITG turbulence[44-46], ion heat diffusivity close to the neoclassical value, an S-curve behaviour of the energy

flux and temperature gradient relation, and a reduction of plasma fluctuations in the experiment. In the FIRE mode, both the fast ion content and fraction (n_f/n_e) are higher in the core region than in the hybrid mode, as shown in Fig. 2c. This is consistent with the higher neutron yield, the outcome of fusion reactions by fast ions shown (Fig. 2a). Therefore, one can conjecture that this ITB is strongly correlated with fast ions in the core region of the plasma. As previously reported, fast ions can stabilise or mitigate microturbulence[8,47-50] such that the transport of thermal ion energy can be reduced at the core region where fast ions are populated.

To study the role of fast ions to the confinement enhancement in the FIRE mode, the time evolution of the fast ion fraction is presented in Fig. 3a, where the location of the ITB, $\rho_{ITB,foot}$, is plotted together to evaluate the correlation between them. Here, $\rho_{ITB,foot}$ is defined as the position where the 2nd derivative of the ion temperature is maximum[25,51]. As shown, the ITB is formed at approximately 3.7 s, where the fast ion fraction is abruptly increased after the second NBI heating. The ITB region exists where the fast ion fraction is high. After applying the third NBI at 5.0 s, the high fast ion fraction area is extended up to ρ_n~0.6, which is followed by expansion of the ITB, where ρ_n is the normalised toroidal flux and depicts a radial position (see fig1a). On the other hand, the fast ion fraction is lower and there is no ITB in the hybrid mode as shown in Fig. 3b. This strong correlation between $\rho_{ITB,foot}$ and the fast ion fraction indicates that fast ions play a role in improving the energy confinement via ITB. The confinement enhancement correlates strongly with suppression of microinstability. Therefore, we next evaluate the effect of fast ions in stabilising the microturbulence using a linear gyrokinetic simulation code, GKW[52]. Fig. 4 presents the GKW simulation results, in which the linear growth rate(γ) of the ITG turbulence, a major contributor to plasma transport[44], can be stabilised by the fast ions. That is, the growth rate which reduces the confinement could be lowered considering the fast ion effects. The stabilisation effects of fast ions are achieved via several physics mechanisms. First, the electromagnetic stabilisation effect, shown as the difference between the solid and dashed lines in Fig. 4a, can be reinforced by fast ions. The electromagnetic fluctuations increase the energy needed for the ITG turbulence to grow compared to the electrostatic fluctuations, and the increase in the plasma pressure by fast ions can lead to larger electromagnetic fluctuations. Second, the Shafranov shift effect, the so-called α-effect, shown as the difference between the solid and dotted lines in Fig. 4b, can also be reinforced by fast ions, where α is , R is the major radius and P is the plasma pressure. The Shafranov shift, the outward radial displacement of the centre of flux surfaces, occurs due to the build-up of the plasma pressure gradient and reduces the vertical drift motion of the plasma driving the turbulence[53]. The fast ions can contribute to the pressure gradient favourable to the Shafranov shift effect. Third, the dilution of the thermal ions and subsequent reduction in the normalised density gradient length, R/L_n, in the core region can suppress the ITG turbulence. The effect is clearly seen as R/L_n decreases in Fig. 4b, where the red closed and black open stars indicate the experimentally relevant reference values with fast ions and assuming no fast ions, respectively. Notably, the effect of ExB flow shear or zonal flows, breaking turbulence eddies and reducing the amplitude of the turbulence fluctuations, is also active in this regime, which can contribute to triggering the ITB[54-57], but thorough analyses are needed with nonlinear simulations in the future. The

fast ion stabilisation effect also plays a role in the hybrid mode[8,49], however, the effect is much lower due to the smaller fraction of fast ions though the hybrid mode shows similar fusion performance with the FIRE mode. Since this core improvement is comparable to the edge improvement in the hybrid mode, they show similar fusion performances. Therefore, we think that the origin of the high performance of this new regime is mainly attributed to the high fraction of fast ions that stabilise the core turbulence, so we coin it the “FIRE mode”.

Since the fast ion fraction is almost constant, the FIRE mode can sustain stationary. This is the result of the balance between the loss and the generation of fast ions. Fast ions are generated mainly from the neutral beams, while there are many loss channels such as thermalization and orbit losses. Because some loss terms can be affected by geometric factors, the extremely low magnetic error field of KSTAR helps to lower the loss rate. Further improvement of the FIRE mode to realize a longer steady-state operation up to 300 s with higher performance is envisaged as one of the promising operation scenarios for a fusion reactor.

Methods

KSTAR

KSTAR[31] is a magnetic fusion device based on the tokamak concept at Korea Institute of Fusion Energy in Daejeon, Republic of Korea. The aim of the project is to develop a steady-state capable advanced superconducting tokamak to establish a scientific and technological basis for ITER and an attractive future fusion reactor. KSTAR is equipped with a fully superconducting magnet system, one of the first tokamaks to feature fully superconducting magnets of great relevance to ITER. The major and the minor radius of KSTAR are 1.8 m and 0.5 m, respectively. The magnetic system consists of 16 niobium-tin direct current toroidal field coils, 10 niobium-tin alternating current poloidal field coils, and 4 niobium-titanium alternating current poloidal field coils[58]. The toroidal field strength is up to 3.5 T at the magnetic axis. KSTAR is equipped with steady-state heating and current drive systems. NBI is the main heating system with the power up to 6 MW and the beam energy up to 100 keV with long-pulse capability up to 300 s. Via highly tangential beam geometry, it can provide the highly efficient current and rotation drive required for high fusion performance plasmas.

Diagnostics

Sets of magnetic diagnostic sensors[59] installed on KSTAR are used to obtain main physics parameters shown in Figs. 1, 2 and Extended Fig. 5 such as the total plasma current, loop voltage, and equilibrium parameters reconstructed by the EFIT code[60]. The magnetic fluctuations drawn in Fig. 1 and Extended Fig. 5 are calculated through Fourier transform from the Mirnov coil measurements[61]. The kinetic profiles presented in Fig. 2c are obtained at the outboard side from Thomson Scattering systems (TS)[62] for the

electron temperature and density and Charge Exchange Spectroscopy (CES)[63] for the impurity Carbon temperature and toroidal velocity. A Two-Colour Interferometer (TCI) with the CO_2 laser and Diode-pumped-solid-state (DPSS) laser[64] and Electron Cyclotron Emission (ECE) measurements are used to determine the electron density and the temperature complementary to the TS measurements. The Motional Stark effect (MSE) diagnostic[65] is employed to extract the core current density profile for the kinetic equilibrium construction. The properties of fast ions are diagnosed through the fast ion loss detector (FILD)[66] and the fast-ion D_α (FIDA)[67]

Experimental Approach

As aforementioned, the plasma configuration is one of the most important components for accessing FIRE mode. It starts from the limited shaping during the plasma current ramping up. Then, the plasma is detached from the inboard side of the device with the USN configuration. As the plasma detached from the inboard side, the plasma density decreased drastically due to the disconnection of the particle source from the inboard side. The threshold power for the H-mode transition follows the 'U-curve' so that the power for the transition increases as the density decreases below the certain value[68]. Therefore, the lower density from the plasma detachment helps to prevent the H-mode transition. Moreover, it is known that the H-mode transition is difficult for the USN configuration where the ion drift direction is away from the X-point. By the combination effect of the lower plasma density and the USN configuration, the H-mode threshold power becomes higher and the plasma cannot enter the H-mode even with high heating power. Note that in some experiments, FIRE mode was obtained even with LSN configuration but the density was kept low ~10^{19} m3 to avoid the H-mode transition. In the experiment, an on-axis NBI system called NBI-1, which lies in the horizontal midplane of device, consists of three positive ion sources, is applied as main auxiliary heating source[69]. Although the maximum total beam power is about 5.5 MW at the maximum beam energy of 100 keV, less input power about 4 MW is injected to avoid H-mode transition while establishing FIRE modes. The electron cyclotron heating (ECH) system[70], the other important additional heating scheme in KSTAR, is applied only for assisting the plasma breakdown. ECH can degrade ITB if it is applied while FIRE mode is obtained.

Power balance analysis

The integrated tokamak modelling suite, TRIASSIC[71], incorporating NUBEAM[72], NCLASS[73], and ASTRA[74], was used for power balance analysis. The NUBEAM code is a Monte Carlo fast ion module to compute the power deposition, driven current, momentum transfer, fuelling, fusion reaction, and so on due to NBI. The NCLASS module is to calculate the neoclassical transport of multi-species in the axisymmetric plasma of the arbitrary aspect ratio, geometry, and collisionality. The ASTRA code is to solve a set of transport equations in toroidal geometry with various physical modules. In this work, NUBEAM is used to

calculate the fast ions and power deposition produced by NBI, NCLASS to calculate the plasma velocity and radial electric field, and ASTRA to calculate the transport equations. The effective charge, Z_{eff} was assumed to be uniform as 1.8[75] dominated by Carbon due to lack of measurements. The radiation power loss was neglected. For FIRE mode, shot 22663 was analysed with full measurements mentioned above. For hybrid mode, shot 22658 was analysed with the electron density and temperature profiles of #22676, a similar discharge to shot 22658, due to lack of TS measurements with the aid of TCI and ECE measurements of shot 22658.

Linear gyrokinetic simulations

The GKW code was used in the linear gyrokinetic analysis for FIRE mode (shot 22663). It simulates microinstabilities and turbulence in a magnetically confined plasma[52]. The most unstable mode of microinstabilities was calculated by GKW for shot 22663 at $\rho = 0.4$ at $t = 5.35$ s with full species assuming the Carbon impurity with $Z_{eff} = 1.8$. The profiles and equilibrium of shot 22663 was obtained from the kinetic equilibrium construction with the MSE diagnostics. In the kinetic equilibrium, fast ions calculated from NUBEAM are considered as an independent species with the equivalent temperature[76]. When fast ions are not considered in the analysis, thermal ions substitute them with the thermal ion temperature. To fix the contribution of electrons in the scanning of thermal ion density gradients, fast ion density gradients are modified to satisfy quasi-neutrality. Collisions are considered in all cases. A full geometry with the Hamada coordinate calculated from CHEASE[77] was used in the GKW simulation.

Analysis of core ITB characteristics

We checked the core ITB characteristics of the FIRE mode in four point of views. Firstly, we evaluated if the normalized ion temperature gradient length, R/L_{Ti} is larger than the ITG threshold value. According to the ITG theory[44-46], it is hard to increase R/L_{Ti} above the critical value of the ITG onset due to the induced anomalous transport, so-called “stiffness”. However, we found that R/L_{Ti} is far above the critical value relaxing stiffness in FIRE mode as shown in extended Fig. 2b. Secondly, we checked the time evolution of the ion heat diffusivity calculated from the power balance analysis. As shown in extended Fig. 2a and Fig. 2c, it is found that the ion heat diffusivity reduces in time correlated with the expansion of ITB though it is still above the neoclassical level. Thirdly, we evaluated the relation between the ion energy flux and the ion temperature gradient to see if any bifurcation exists in time and space. As shown in extended Fig. 3, the normalised ion energy flux draws a “S-curve” in the 3-D landscape of the flux-gradient space[78]. The reduction of the energy flux while the gradient increases implies a transport bifurcation, known to be an ITB characteristic. This bifurcation occurs at where the ITB foot locates when the ITB was thought to be formed. Lastly, the amplitude of electron temperature fluctuations measured by electron cyclotron emission imaging (ECEI) decreases as ion energy confinement is improved as shown in Extended Fig. 4.

This implies the reduction of turbulence persisting in the plasma from the breakdown[79]. As the ITB location expands to , the fluctuation is severely reduced implying stabilisation of turbulence. Based on the analysis above, an ITB is thought to be formed in the core region of FIRE mode by stabilisation of the ITG turbulence.

Analysis of edge characteristics

Some of FIRE modes have plasma edge characteristics similar to that of I-mode[80-84] in which ETB is formed only in the energy channel not in the particle channel. It is noteworthy that I-modes are typically obtained with USN configurations with the ion ∇B drift direction away from X-point which is similar to the experimental condition of FIRE mode. Therefore, operations with the USN configuration could have potential to establish I-mode at the edge with the auxiliary heating power close to the H mode transition in FIRE mode. In I-modes, the edge particle transport remains turbulent due to the weakly coherent modes so that the pressure gradient is reduced and subsequently ELMs are prevented. Similarly, FIRE modes with I-mode like edge shows a high ion temperature gradient at the edge region and no clear barrier in the density profile. Therefore, no ELMs are observed as shown in the Dα signal in Fig. 2a. Extended Fig. 5 presents an example of FIRE mode with an I-mode like edge, where a weakly coherent mode appears in the Mirnov coil signal. The absence of the particle transport barrier can enhance the fraction of fast ions by reducing thermalisation of fast ions with a low density so to sustain high performance in FIRE modes. Note that no ITBs seem to present in I-modes developed so far.

Statistical analysis of internal inductance

The plasma performance (β_N, H_{89}) and the internal inductance (l_i) were gathered to find characteristic regime of FIRE mode for stationary discharges in three kinds of plasmas. One is FIRE mode with diverted configuration and low density. Another is H-mode with diverted configuration and high density. The other is plasma with limited configuration including some normal ITB discharges in KSTAR. The plasma internal inductance of FIRE modes is $l_i > 1.25$ higher than H-modes implying more peaked current density profiles with monotonic q-profiles with the central q-value above or close to unity. This is a distinguished feature compared with conventional ITB discharges with reversed magnetic shear[27,28,85]. High performing FIRE modes with $\beta_N > 2.0$ and $H_{89} > 2.0$ are located on the relatively low l_i window as a result of a broader ITB and/or a presence of a transport barrier-like structure in the edge region. It is anticipated that FIRE mode can be further enhanced by broadening the ITB and strengthen the ETB.

Data availability

Raw data were generated from the KSTAR team. The data that support the findings of this study are available from the corresponding author upon reasonable request.

Declarations

Acknowledgements

The authors would like to express our gratitude for fruitful discussions with R. Nazikianat Princeton Plasma Physics Laboratory, H. Zohm at Max-Plank-Institute for Plasma Physics and Wonho Choe at Korea Advanced Institute of Science and Technology. This work was supported by Ministry of Science and ICT under KFE R&D Program of "KSTAR Experimental Collaboration and Fusion Plasma Research(KFE-EN2101-12)". Also, this research was supported by National R&D Program through the National Research Foundation of Korea (NRF) funded by the Ministry of Science & ICT (NRF-2021M1A7A4091135). The authors gratefully acknowledge The Research Institute of Energy and Resources and The Institute of Engineering Research at Seoul National University.

Author contributions

Y.-S. Na, H. Han, J. Chung, Y.H. Lee, S.J. Park, Y.S. Park conceived the experiments.

H. Han, J. Chung, J. Kang, S.H Hahn, H.S. Kim, S.J. Park, Y.H. Lee, and Y.-S. Na conducted all experiments controlling the plasma as designed.

W.H. Ko and J.K. Lee diagnosed the ion temperature in the experiments using the CES.

K.D. Lee diagnosed the electron temperature in the experiments using the ECE.

J. Ko diagnosed the radial magnetic pitch angle profile using the MSE.

J. Jang measured the emission lines from neutralizing of ion species to diagnose the impurity intensity as well as the plasma interaction.

K.C. Lee diagnosed the plasma density using the TCI.

J.H. Kim diagnosed the fast ion properties using FILD and FIDA.

M.J. Choi and J.H Lee diagnosed the temperature fluctuation using the ECEI.

H. Han, S.J Park, J.M. Seo, B. Kim, J. Gwak, M.S. Cha, J.-K. Park, and Y.-S. Na prepared the manuscript and figures.

S.J Park, Y.H. Lee, C.Y. Lee, and G.J. Choi performed the power balance and linear gyrokinetic simulations.

T.S. Hahm, J.P. Lee, C.K. Sung, S.M. Yang and S.K. Kim, and Y.-S. Na analysed the simulation results.

W.C. Kim and S.W. Yoon supported all of this work as the project managers.

Y.-S. Na designed and led the whole research.

All authors analysed the results and contributed to the compilation and review of the manuscript.

Reference

1. Banacloche, S., Gamarra, A. R., Lechon, Y., Bustreo, C. Socioeconomic and environmental impacts of bringing the sun to earth: A sustainability analysis of a fusion power plant deployment. *Energy* **209**, 118460 (2020).

2. Wesson, J. *Tokamaks* 4th edn, Ch. 1, 2-27 & Ch. 13, 764-767 (Oxford Univ. Press, Oxford, 2011).

3. Wagner, F. et al. Regime of Improved Confinement and High Beta in. Neutral-Beam-Heated Divertor Discharges of the ASDEX Tokamak. *Phys. Rev. Lett.* **49,** 1408-1412 (1982).

4. Shimada, M. et al. Progress in the ITER physics basis - Chapter 1: Overview and summary. *Nucl. Fusion* **47**, S1-S17 (2007).

5. Barbarino, M. A brief history of nuclear fusion. *Nat. Phys.* **16**, 890–893 (2020).

6. The way ahead for fusion. *Nat. Phys.* **16**, 889 (2020).

7. Reichert, S. Inside ITER. *Nat. Phys.* **16**, 895 (2020).

8. Na, Y. S. et al. On hybrid scenarios in KSTAR. *Nucl. Fusion **60***, 086006 (2020).

9. Luce T. C. et al. Development of advanced inductive scenarios for ITER. *Nucl. Fusion* **54**, 013015 (2014).

10. Y. Kamada et al., Long sustainment of JT-60U plasmas with high integrated performance. *Nucl. Fusion* **39** 1845 (1999).

11. Ferron J. R. et al., Progress toward fully noninductive discharge operation in DIII-D using off-axis neutral beam injection. *Phys. Plasmas* **20**, 092504 (2013).

12. Yoon, S.W. et al. Characteristics of the first H-mode discharges in KSTAR. *Nucl. Fusion* **51,** 113009 (2011).

13. Li, J., Guo, H. & Wan, B. et al. A long-pulse high-confinement plasma regime in the Experimental Advanced Superconducting Tokamak. *Nat. Phys.* **9**, 817–821 (2013).

14. Keilhacker, M. et al. Confinement studies in L and H-type Asdex discharges. *Plasma Phys. Control. Fusion* **26,** 49-63 (1984).

15. Zohm, H. et al. Edge localized modes (ELMs). *Plasma Phys. Control. Fusion* **38,** 105-128 (1996).

16. Lang, P. T. et al. ELM frequency control by continuous small pellet injection in ASDEX Upgrade. *Nucl. Fusion* **43**, 1110-1120 (2003).

17. Degeling, A.W. et al. Magnetic triggering of ELMs in TCV. *Plasma Phys. Control. Fusion* **45**, 1637-1655 (2003).

18. Evans, T. E. et al. Suppression of Large Edge-Localized Modes in High-Confinement DIII-D Plasmas with a Stochastic Magnetic Boundary. *Phys. Rev. Lett.* **92**, 235003 (2004).

19. Evans, T. E. et al. Edge stability and transport control with resonant magnetic perturbations in collisionless tokamak plasmas. *Nat. Phys.* **2**, 419–423 (2006).

20. Jeon, Y. M. et al. Suppression of Edge Localized Modes in High-Confinement KSTAR Plasmas by Nonaxisymmetric Magnetic Perturbations. *Phys. Rev. Lett.* **109**, 035004 (2012).

21. Park, J.-K. et al. 3D field phase-space control in tokamak plasmas. *Nat. Phys.* **14**, 1223–1228 (2018).

22. Loarte, A. et al. Progress on the application of ELM control schemes to ITER scenarios from the non-active phase to DT operation. *Nucl. Fusion* **54**, 033007 (2014).

23. Burrell, K. H. Effects of E×B velocity shear and magnetic shear on turbulence and transport in magnetic confinement devices. *Phys. Plasmas* **4**, 1499 (1997).

24. Conway, G. D. et al., Suppression of Plasma Turbulence During Optimized Shear Configurations in JET, *Phys. Rev. Lett.* **84**, 1463 (2000)

25. Chung, J. et al. Formation of the internal transport barrier in KSTAR. *Nucl. Fusion* **58**, 016019 (2018).

26. Koide, Y. et al. Internal transport barrier on q=3 surface and poloidal plasma spin up in JT-60U high-β_p discharges. *Phys. Rev. Lett.* **72**, 3662 (1994).

27. Levinton, F. M. et al. Improved Confinement with Reversed Magnetic Shear in TFTR. *Phys. Rev. Lett.* **75**, 4417 (1995).

28. Strait, E. J. et al. Enhanced Confinement and Stability in DIII-D Discharges with Reversed Magnetic Shear. *Phys. Rev. Lett.* **75**, 4421 (1995).

29. Tardini, G. et al. Thermal ions dilution and ITG suppression in ASDEX Upgrade ion ITBs. *Nucl. Fusion* **47**, 280 (2007).

30. Park, H. K. & Sabbagh, S. A. Effect of the neutral beam fuelling profile on fusion power, confinement and stability in TFTR. *Nucl. Fusion* **37**, 629–42 (1997).

31. Lee, G. S. et al. Design and construction of the KSTAR tokamak. *Nucl. Fusion* **41**, 1515 (2001).

32. Yushmanov, P. N. et al. Scalings for tokamak energy confinement. *Nucl. Fusion* **30**, 1999 (1990).

33. Crisanti, F. et al. JET Quasistationary Internal-Transport-Barrier Operation with Active Control of the Pressure Profile. *Phys. Rev. Lett.* **88**, 145004 (2002).

34. Manickam, J. et. al. Ideal MHD stability properties of pressure driven modes in low shear tokamaks. *Nucl. Fusion* **27**, 1461 (1987).

35. Chu, M. S. et al. Resistive Interchange Modes in Negative Central Shear Tokamaks with Peaked Pressure Profiles. *Phys. Rev. Lett.* **77**, 2710 (1996).

36. Okabayashi, M. et. al. Mode structure of disruption precursors in TFTR enhanced reversed shear discharges. *Nucl. Fusion* **38**, 1149 (1998).

37. de Vries, P. C. et al. Survey of disruption causes at JET. *Nucl. Fusion* **51**, 053018 (2011).

38. ITER Research Plan within the Staged Approach. ITER Technical Report ITR-18-003 (2018).

39. Hollmann, E. M. et al. Status of research toward the ITER disruption mitigation system. *Phys. Plasmas* **22**, 021802 (2015).

40. Strait, E. J. Stability of high beta tokamak plasmas. *Phys. Plasmas* **1**, 1415 (1994)

41. Chapman, I. T. et al. Analysis of high β regimes for DEMO. *Fusion Eng. Des.* **86**, 141-150 (2011)

42. Giruzzi, G. et al. Modelling of pulsed and steady-state DEMO scenarios. *Nucl. Fusion* **55**, 073002 (2015)

43. Kim, H.-S. et al. Characteristics of global energy confinement in KSTAR L- and H-mode plasmas. *Nucl. Fusion* **54**, 083012 (2014).

44. Conner, J. W. & Wilson, H. R. Survey of theories of anomalous transport. *Plasma Phys. Control. Fusion* **36**, 719 (1994).

45. Hahm, T. S. & Tang, W. M. Properties of ion temperature gradient drift instabilities in H-mode plasmas. *Phys. Plasmas* **1**, 1185 (1989).

46. Guo S.C. & Romanelli F. The linear threshold of the ion-temperature-gradient-driven mode. *Phys. Plasmas* **5**, 520 (1993).

47. Citrin, J. et al. Nonlinear Stabilization of Tokamak Microturbulence by Fast Ions. *Phys. Rev. Lett.* **111**, 155001 (2013).

48. Romanelli, M. et al. Fast ion stabilization of the ion temperature gradient driven modes in the Joint European Torus hybrid-scenario plasmas: a trigger mechanism for internal transport barrier formation.

Plasma Phys. Control. Fusion **52**, 045007 (2010).

49. Garcia, J. et al. Key impact of finite-beta and fast ions in core and edge tokamak regions for the transition to advanced scenarios. *Nucl. Fusion* **55**, 053007 (2015).

50. Di Siena, A. et al. Nonlinear electromagnetic interplay between fast ions and ion-temperature-gradient plasma turbulence. *J. Plasma Phys.* **87**, 555870201 (2021).

51. Connor, J.W. et al. A review of internal transport barrier physics for steady-state operation of tokamaks. *Nucl. Fusion* **44**, R1–R49 (2004)

52. Peeters, A. G. et al. The nonlinear gyro-kinetic flux tube code GKW. *Comput. Phys. Commun.* **180**, 2650 (2009).

53. Bourdelle, C. et al. Impact of the α parameter on the microstability of internal transport barriers. *Nucl. Fusion* **45**, 110 (2005).

54. Hahm T.S. & Burrell K.H. Flow shear induced fluctuation suppression in finite aspect ratio shaped tokamak plasma. *Phys. Plasmas* **2**, 1648 (1995).

55. Burrell, K. H. Effects of E×B velocity shear and magnetic shear on turbulence and transport in magnetic confinement devices. *Phys. Plasmas* **4**, 1499 (1997).

56. Greenfield C.M. et al. Transport and performance in DIII-D discharges with weak or negative central magnetic shear. *Phys. Plasmas* **4**, 1596 (1997).

57. Kamada, Y. Observations on the formation and control of transport barriers. *Plasma Phys. Control. Fusion* **42**, A65 (2000).

58. Kim, K. et al. Status of the KSTAR superconducting magnet system development. *Nucl. Fusion* **45**, 783 (2005).

59. Lee, S. G. et al. Magnetic diagnostics for the first plasma operation in Korea Superconducting Tokamak Advanced Research. *Rev. Sci. Instrum.* **79**, 10F117 (2008).

60. Lao, L.L. et al. Reconstruction of current profile parameters and plasma shapes in tokamaks. *Nucl. Fusion* **25**, 1611 (1985).

61. Bak, J. G. et al. Initial measurements by using Mirnov coils in the KSTAR machine. in *Proc. 37th EPS Conference on Plasma Physics*, p. 5.102. (2010).

62. Lee, J. H. et al. Edge profile measurements using Thomson scattering on the KSTAR tokamak. *Rev. Sci. Instrum.* **85**, 11D407 (2014).

63. Ko, W. H. et al. Rotation characteristics during the resonant magnetic perturbation induced edge localized mode suppression on the KSTAR. *Rev. Sci. Instrum.* **85**, 11E413 (2014).

64. Juhn, J.-W. et al. Multi-chord IR–visible two-color interferometer on KSTAR. *Rev. Sci. Instrum.* **92**, 043559 (2021).

65. Chung, J. et al. Instrumentation for a multichord motional Stark effect diagnostic in KSTAR. *Rev. Sci. Instrum.* **85**, 11D827 (2014).

66. Junghee Kim et al., Initial measurements of fast ion loss in KSTAR, *Rev. Sci. Instrum.* **83**, 10D305 (2012)

67. J.W. Yoo et al., Fast-ion Dα spectroscopy diagnostic at KSTAR, *Rev. Sci. Instrum., **92**, 043504 (2021)*

68. Ahn, J.-W. et al, Confinement and ELM characteristics of H-mode plasmas in KSTAR. *Nucl. Fusion* **52**, 114001 (2012).

69. Jeong, S. H. et al. First neutral beam injection experiments on KSTAR tokamak. *Rev. Sci. Instrum.* **83**, 02B102 (2012)

70. Wang, S. J. et al. Recent experimental results of KSTAR RF heating and current drive. *AIP Conf. Proc.* **1689**, 030014 (2015).

71. Lee, C. Y. et al. Development of Integrated Suite of Codes and Its Validation on KSTAR. *28th IAEA Fusion Energy Conference* (2021).

72. Pankin, A. et al. The tokamak Monte Carlo fast ion module NUBEAM in the National Transport Code Collaboration library. *Phys. Commun.* **159**, 157 (2004).

73. Houlberg, W. A. et al. Bootstrap current and neoclassical transport in tokamaks of arbitrary collisionality and aspect ratio. *Physics of Plasmas* **4**, 3230 (1997).

74. Pereverzev G. et al. Automated System for TRansport Analysis. *IPP-Report IPP 5/98* (2002).

75. Sarwar, S. et al. Effective ion charge (Z_{eff}) measurements and impurity behaviour in KSTAR. *Rev. Sci. Instrum.* **89**, 043504 (2018).

76. Angioni, C. & Peeters, A. G. Gyrokinetic calculations of diffusive and convective transport of α particles with a slowing-down distribution function. *Phys. Plasmas* **15**, 052307 (2008).

77. Lutjens H., Bondeson A. & Sauter O. The CHEASE code for toroidal MHD equilibria. *Comput. Phys. Commun.* **97**, 219 (1996).

78. P. H. Diamond et al. On the Dynamics of Transition to Enhanced Confinement of Reversed Magnetic Shear Discharges. *Phys. Rev. Lett.* **78**, 1472-1475 (1997)

79. Yoo, M. G., Lee, J. & Kim, Y. G. et al. Evidence of a turbulent ExB mixing avalanche mechanism of gas breakdown in strongly magnetized systems. *Nat Commun* **9**, 3523 (2018).

80. McDermott, R. M. et al. Edge radial electric field structure and its connections to H -mode confinement in Alcator C-Mod plasmas. Phy. Plasmas **16**, 056103 (2009).

81. Whyte, D.G. et al. I-mode: an H-mode energy confinement regime with L-mode particle transport in Alcator C-Mod. *Nucl. Fusion* **50**, 105005 (2010).

82. Manz, P. et al. Geodesic oscillations and the weakly coherent mode in the I-mode of ASDEX Upgrade. *Nucl. Fusion* **55**, 083004 (2015).

83. Marinoni, A. et al. Characterization of density fluctuations during the search for an I-mode regime on the DIII-D tokamak. *Nucl. Fusion* **55**, 093019 (2015).

84. Ryter, F. et al. I-mode studies at ASDEX Upgrade: L-I and I-H transitions, pedestal and confinement properties. *Nucl. Fusion* **57**, 016004 (2017)

85. Fujita, T. et al. Plasma Equilibrium and Confinement in a Tokamak with Nearly Zero Central Current Density in JT-60U. *Phys. Rev. Lett.* **87**, 245001 (2001)

Figures

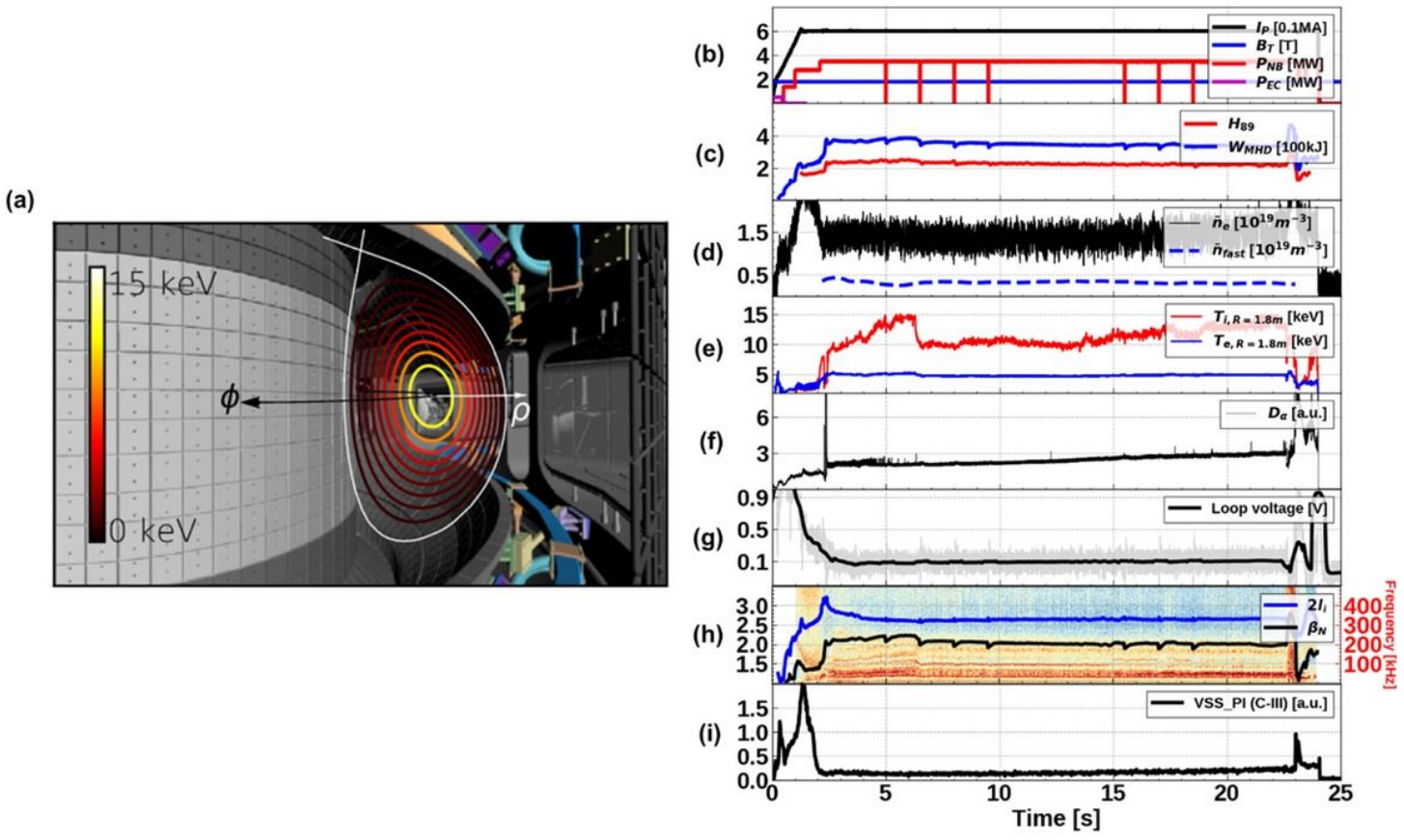

Figure 1

(a) Plasma configuration of a FIRE mode in Korea Superconducting Tokamak Advanced Research (KSTAR). The colour of lines indicates the ion temperature in keV. 1 keV corresponds to ~120 million Kelvin. Time evolution of main physics and engineering parameters; (b) plasma current (Ip), toroidal magnetic field strength at the magnetic axis (BT), neutral beam power (PNBI), and electron cyclotron resonance heating power (PECH), (c) energy confinement ratio to the ITER89 scaling law (H89) and stored plasma energy (WMHD), (d) line-averaged electron density (ne) and line-averaged fast ion density (nfast), (e) ion and electron temperature at R = 1.8 m (Ti R=1.8m and Te R=1.8m), (f) Dα emission intensity, (g) loop voltage, (h) internal inductance (li), normalised beta (βN), and the magnetic fluctuations detected by Mirnov coils, (i) Carbon line radiation intensity from C2+→3+.

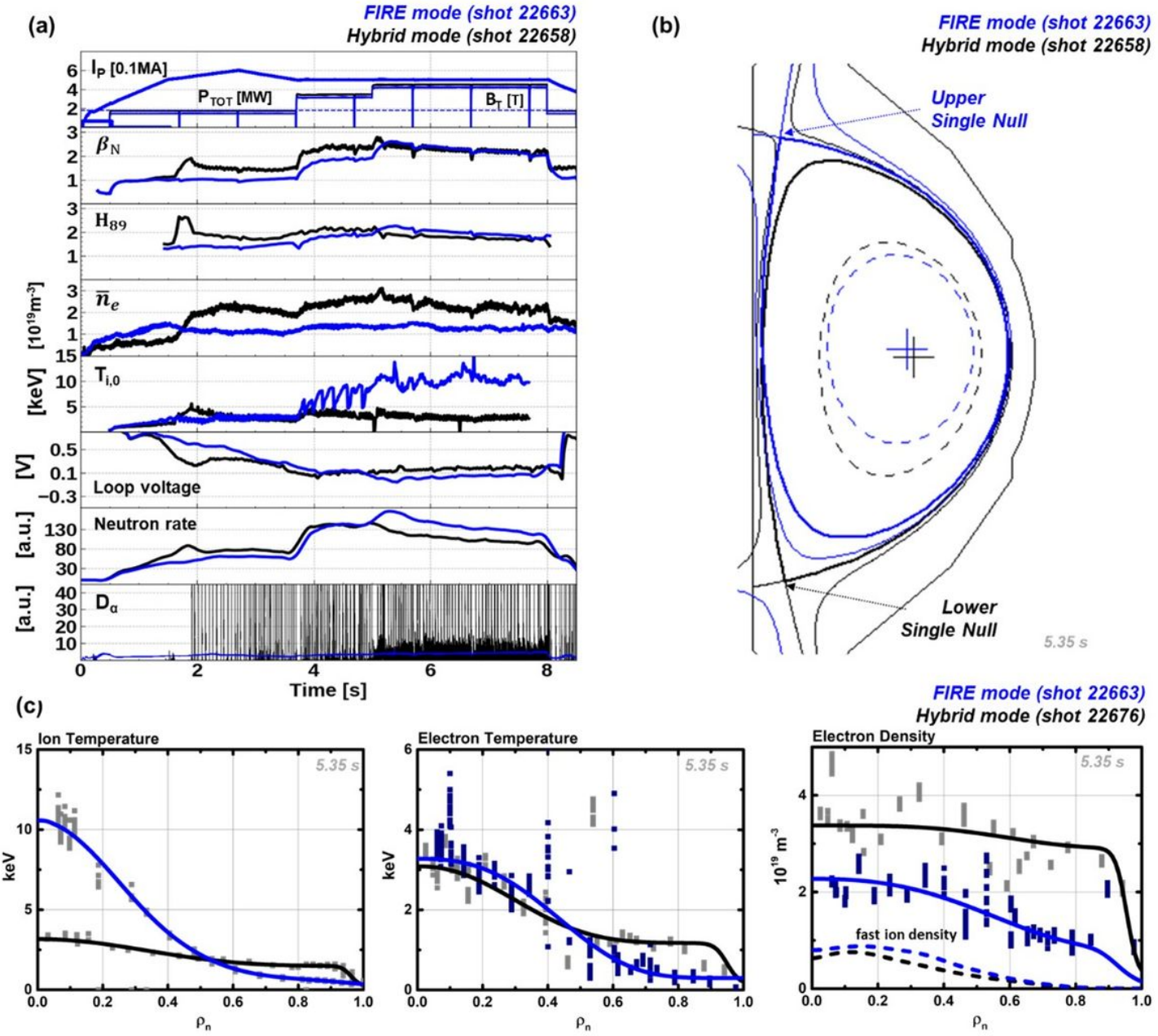

Figure 2

(a) Comparison of the time evolution of main plasma parameters between a FIRE mode and a hybrid mode. (b) The plasma configuration; USN in FIRE mode, LSN in hybrid mode. (c) Ion and electron temperature profile and electron density profile of FIRE mode and hybrid mode in normalised toroidal flux, ρn at 5.35 s. The time is indicated as the vertical dashed line in (a).

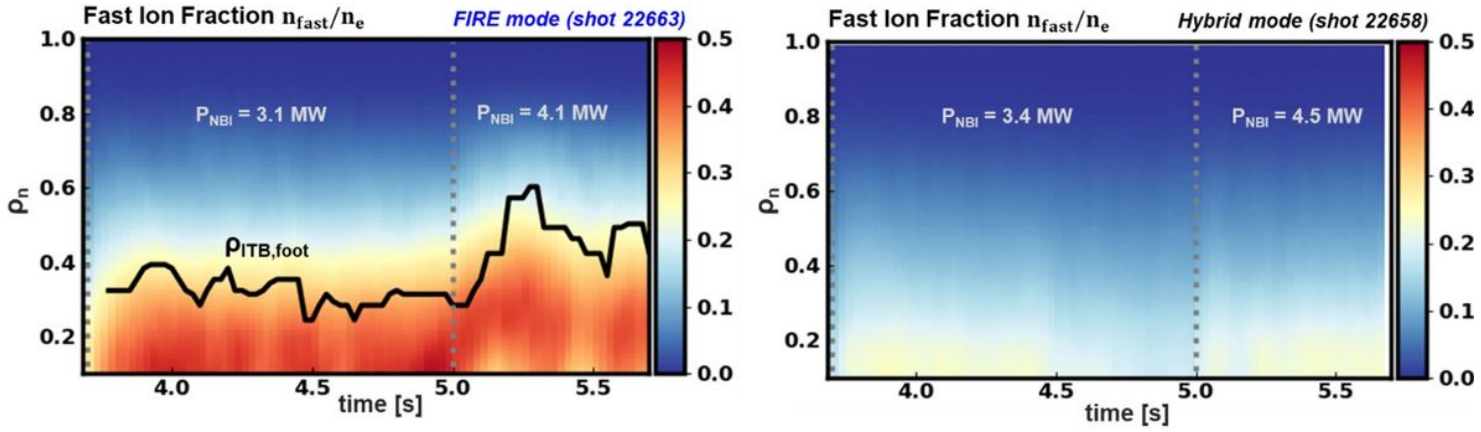

Figure 3

The time evolution of the fraction of the fast ion density to the electron density, nfast/ne in a FIRE mode (a) and a hybrid mode (b). The characteristic location of core confinement improvement, ρ_(ITB,foot) (ITB foot location where the 2nd derivative of the ion temperature profile is maximised), is plotted in the black line. The NBI heating power is increased from ~3 MW to ~4 MW at 5.0 s indicated as the gray vertical dashed line.

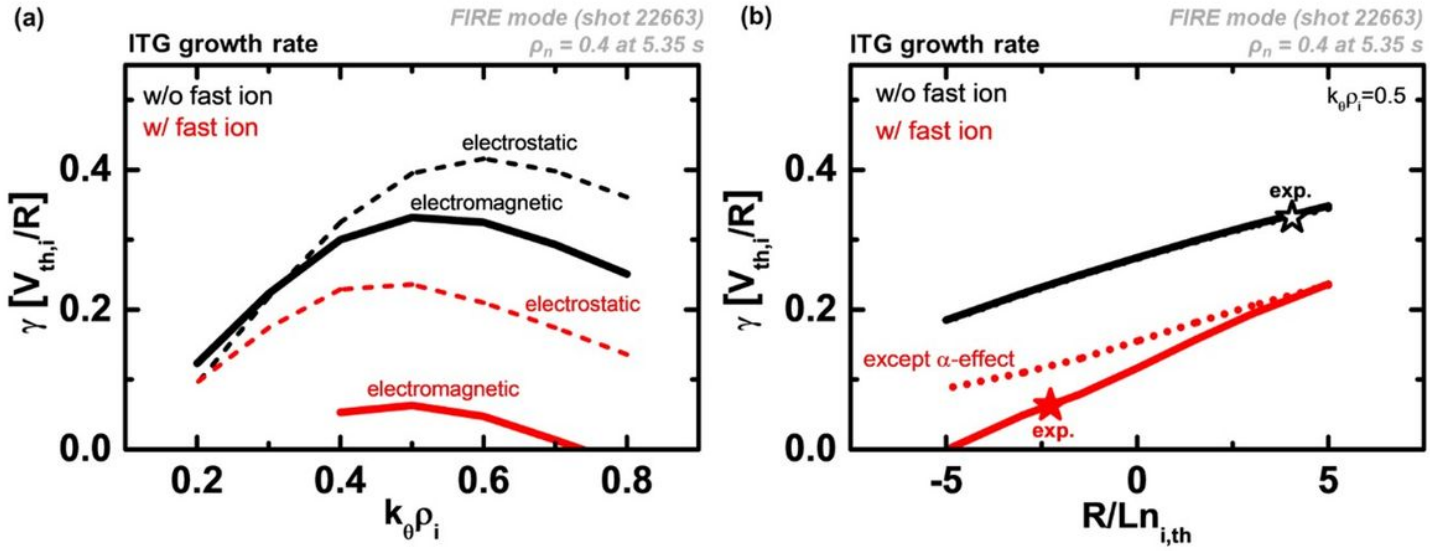

Figure 4

The linear gyrokinetic simulation results with the GKW code; (a) the ITG growth rate versus kθρi with electrostatic (dashed lines) and electromagnetic (solid lines) simulations with (red) and without (black) considering the fast ions. The fast ions are substituted by thermal ions when they are not considered. (b) the ITG growth rate versus the normalised thermal ion density gradient length with (red) and without

(black) considering the fast ion for kθρi = 0.5 exhibiting the maximum growth rate in (a). Here kθ and ρi are the poloidal wave number and the ion Larmor radius, respectively. The black open and the red closed star in (b) represent the reference experimental value without and with fast ions, respectively. The thermal ion density gradient is the same as the total ion density gradient for the case without fast ions. Excluding the α-effect is compared for the case with the fast ion, shown as the red dotted line in (b), where α is -q^2 βR∇P/P. Simulations are performed at ρn = 0.4 at 5.35 s in FIRE mode (shot 22663).

Supplementary Files

This is a list of supplementary files associated with this preprint. Click to download.

- ExtendedMovie1.mp4
- ExtendedFiles.docx